ADP–16–42/T998
CoEPP–MN–16–29

Dark matter candidates in the constrained Exceptional Supersymmetric Standard Model

P. Athron[a,1], A.W. Thomas[b], S.J. Underwood[b,2], M.J. White[b,3]

[a] *ARC Centre of Excellence for Particle Physics at the Terascale, School of Physics & Astronomy, Monash University, Melbourne VIC 3800, Australia*

[b] *ARC Centre of Excellence for Particle Physics at the Terascale and CSSM, School of Physical Sciences, The University of Adelaide, Adelaide SA 5005, Australia*

[1] *peter.athron@coepp.org.au*

[2] *sophie.underwood@adelaide.edu.au*

[3] *martin.white@adelaide.edu.au*

arXiv:1611.05966v1 [hep-ph] 18 Nov 2016

Abstract

The Exceptional Supersymmetric Standard Model (E_6SSM) is a low energy alternative to the MSSM with an extra $U(1)$ gauge symmetry and three generations of matter filling complete 27-plet representations of E_6. This provides both new D and F term contributions that raise the Higgs mass at tree level, and a compelling solution to the μ-problem of the MSSM by forbidding such a term with the extra $U(1)$ symmetry. Instead, an effective μ-term is generated from the VEV of an SM singlet which breaks the extra $U(1)$ symmetry at low energies, giving rise to a massive Z'. We explore the phenomenology of the constrained version of this model (cE_6SSM) in substantially more detail than has been carried out previously, performing a ten dimensional scan that reveals a large volume of viable parameter space. We classify the different mechanisms for generating the measured relic density of dark matter found in the scan, including the identification of a new mechanism involving mixed bino/inert-Higgsino dark matter. We show which mechanisms can evade the latest direct detection limits from the LUX 2016 experiment. Finally we present benchmarks consistent with all the experimental constraints and which could be discovered with the XENON1T experiment.

I. INTRODUCTION

With the discovery of a 125 GeV Higgs boson, all elementary particles in the Standard Model (SM) of particle physics have been discovered and the model is extremely well verified as a description of nature, fitting observations from past and current collider experiments. However, the SM cannot explain the observed dark matter, which constitutes 23% of the universe's mass-energy content and has motivated many proposed modifications to the SM. Supersymmetric extensions in particular, although motivated for many other reasons, are also often favoured for providing viable Weakly Interacting Massive Particle (WIMP) candidates for dark matter. For instance, the application of R-parity, a Z_2 symmetry meant to preserve baryon and lepton number, to the Minimal Supersymmetric Standard Model (MSSM) ensures the stability of the lightest supersymmetric particle.

However the MSSM now requires considerable fine tuning to obtain a Higgs mass of 125 GeV and it has a so-called "μ problem" associated with it. The coupling between the Higgs superfields, μ, is the only dimension one parameter in the MSSM superpotential. Since, for phenomenological reasons, μ should be of the same order of magnitude as the electroweak (EW) scale, despite there being no physical connection between them, this presents a naturalness problem.

Here we investigate dark matter in a well motivated E_6-inspired model. We explore the different types of neutralino dark matter that can explain the observed relic density, while satisfying collider constraints and examine the impact of recent direct detection experiments on the model. E_6-inspired supersymmetric models [1, 2] provide a solution to the μ problem wherein the μ-term is forbidden by an extra $U(1)$ gauge symmetry which appears from the breakdown of E_6 and survives to low energies, where it is broken close to scale of electroweak symmetry breaking. The break down of this extra $U(1)$ symmetry occurs when an SM singlet picks up a VEV, dynamically generating an effective μ-term without the accompanying domain wall / tadpole problems that appear in the NMSSM [3, 4].

E_6-inspired models with an extra $U(1)$ gauge symmetry have attracted extensive interest in the literature [5–29]. Here we work specifically with a $U(1)_N$ gauge symmetry at low energies under which the right handed neutrino remains interactionless. This is used in the Exceptional Supersymmetric Standard Model (E_6SSM) [30–32] and closely related models [33–38] to allow right-handed neutrinos to gain mass far above the TeV scale and trigger a see-saw mechanism that explains the tiny observed masses of neutrinos. This can also provide a leptogenesis mechanism to explain the baryon asymmetry in the Universe [39, 40].

The gauge coupling running in the E_6SSM at the two-loop level leads to unification more precisely than in the MSSM [41], while in slightly modified scenarios two-step unification can take place [33, 42]. If the exotic particles are light in these models this can open up non-standard decays of the SM–like Higgs

boson [38, 43, 44]. In the constrained version of the E_6SSM, the particle spectrum, collider signatures and fine tuning have been studied [45–50]. The threshold corrections to the $\overline{DR}$ gauge and Yukawa couplings in the E_6SSM were calculated and the numerical impact in the constrained version examined [51, 52]. The impact of gauge kinetic mixing in the case where both the extra U(1)'s appearing from the breakdown of E_6 are present at low energy was studied in [53]. The E_6SSM was also included in studies looking at how first or second generation sfermion masses can be used to constrain the GUT scale parameters [54] and the renormalization of VEVs [55, 56]. Very recently the model has been studied in the context of electroweak baryogenesis [57] and the possibility of it explaining the recent apparent diphoton excess was also discussed [58–60].

The situation for dark matter in these models can be quite different from that of the MSSM. The E_6SSM neutralino sector is extended compared to the MSSM by the both extra matter fields and the fermion component from the extra vector superfield associated the extra $U(1)$. If only this new gaugino and the third generation singlino (superpartner of the singlet Higgs field which breaks the extra $U(1)$ symmetry) mix with the MSSM-like gauginos and Higgsinos, then the neutralino sector would be that of the $U(1)$-extended Supersymmetric Standard Model (USSM) [61].

However if one considers interactions from $27_i \times 27_j \times 27_k$ then the superpotential will have a term amongst the Higgs-like fields analogous to that of the NMSSM, but with indices running over all three generations,

$$\Sigma_{ijk}\lambda_{ijk}S_i H_j^d H_k^u \in W_{E6SSM}, \qquad i,j,k \in (1,2,3). \tag{1}$$

As will be discussed later, the first two generations of Higgs-like fields will remain inert and will not develop a VEV, while the 3rd generation will be the actual Higgs fields, with the neutral scalar components developing VEVs. The effective μ parameter is then provided by $\mu_{eff} = \frac{s\lambda_{333}}{\sqrt{2}}$, where s is the VEV for the singlet scalar field S_3.

Such an interaction allows mixing between the Higgsinos and singlino (i.e. the superpartners of the actual Higgs fields) and the "inert" Higgsinos and "inert" singlino which are the fermion components of the inert first and second generation Higgs-like superfields. Indeed, scenarios where the correct relic density can be obtained entirely from the inert sector have been explored [62]. However because the "inert" singlinos are always rather light states, these scenarios are now ruled out by limits on non-standard Higgs decays and direct detection of dark matter experiments such as LUX [63–65]. Dark matter has also been studied in a related E_6 model where there is a single, exact custodial symmetry that decouples all of the "inert" neutralinos from the USSM-like neutralino states, rendering the dark matter situation much more similar to that of the MSSM [66, 67].

In this article we instead consider specifically the EZSSM [68] scenario, where only the light singlino

states have been decoupled from the rest of the neutralino sector and contribute negligibly to the dark matter relic density. Only specific scenarios with bino-like dark matter candidates have been examined for this previously. In those scenarios the relic density is explained through a new mechanism that involves the bino scattering off SM states into inert-Higgsinos, where the latter need to have masses very close to that of the bino for this to work. However, we will show that the model has a much richer set of possibilities for obtaining the measured relic density of dark matter.

Here we expand substantially on previous work exploring the parameter space of the E_6SSM [46–50]. For the first time we include the relic density calculation in a systematic exploration of the parameter space of the model. Furthermore, we vary the full set of parameters in the constrained model, rather than just a two or three dimensional subset. This includes varying Z_2^H violating Yukawa couplings that mix the exotic neutralino (i.e. the inert-Higgsino) couplings with the USSM sector neutralinos formed by the bino, wino, Higgsinos and fermion components of the gauge and singlet supermultiplets.

With this more systematic approach we reveal the different possible neutralino dark matter scenarios that can explain the relic density. We find that the dark matter candidate can be predominantly bino, Higgsino or inert-Higgsino in nature, or it can have a significant mixture of two or all three of these. In particular, the scenarios involving a significant inert-Higgsino dark matter admixture have not been discussed before in any E_6-inspired model. Scenarios with a significant admixture of inert-Higgsino and bino are very interesting as these scenarios can fit the relic density without driving the spin-independent cross-section up, as happens in the MSSM and E_6-inspired models where the dark matter candidate has substantial admixtures of Higgsino and bino.

We also show that it is possible to fit the relic density of dark matter simultaneously with collider data, such as the 125 GeV Higgs mass and other limits from collider experiments, across a wide range of parameters. We present new benchmarks from the scans which can do this and represent the different types of dark matter that we have identified.

This paper is structured as follows. In Section II we review the model with particular focus on the neutralino sector. In Section III we outline our scan procedure. In Section IV we show the results of scans of the parameter space which reveal that a large volume of the parameter space is consistent with all available data and the limits from direct detection on the exotic couplings. We then identify the characteristics of the new dark matter candidates and present a set of benchmark points for scenarios that survive the latest limits from direct detection experiments. Finally we present our conclusions in Section V.

II. E_6SSM

The breakdown of E_6 can lead to two extra $U(1)$ gauge groups defined by the breaking of $E_6 \rightarrow SO(10) \times U(1)_\psi$, and the subsequent breaking of $SO(10)$ into $SU(5)$, $SO(10) \rightarrow SU(5) \times U(1)_\chi$ (this is reviewed in e.g. [69]). In E_6-inspired models that solve the μ problem, one linear combination survives to low energies and, in the E_6SSM, this combination is

$$U(1)_N = \frac{1}{4}U(1)_\chi + \frac{\sqrt{15}}{4}U(1)_\psi. \tag{2}$$

The full low energy gauge group of the E_6SSM is then

$$SU(3)_C \times SU(2)_W \times U(1)_Y \times U(1)_N. \tag{3}$$

This is subsequently broken down to $SU(3)_C \times U(1)_e$ when the Higgs fields that couple to up-type fermions, H_u, down-type fermions, H_d, and the singlet Higgs field, S, pick up VEVs.

The E_6SSM has an extended particle content to include three complete 27_i representations of E_6 (where i runs from 1 to 3). This ensures the cancellation of gauge anomalies in each generation. The three families decompose as:

$$27_i \rightarrow (10,1)_i + (5^*,2)_i + (5^*,-3)_i + (5,-2)_i + (1,5)_i + (1,0)_i, \tag{4}$$

where the first quantity in each bracket is the $SU(5)$ representation and the second quantity is the extra $U(1)_N$ charge (the decomposition occurs under a $SU(5) \times U(1)_N$ subgroup of E_6). The first two terms contain quarks and leptons, the third and fourth terms contain up- and down-type Higgs-like doublets H_i^u and H_i^d as well as additional exotic coloured states D_i and $\bar{D}_i$, the fifth contains the SM-singlet fields S_i and the last contains the right-handed neutrinos.

The matter content is then completed with the inclusion of two additional $SU(2)$ multiplets H' and $\overline{H}'$, which are the only components from additional $27'$ and $\overline{27}'$ that survive to low energies. These incomplete multiplets at low energies ensure that gauge coupling unification can be achieved. The low energy matter content of the model looks like,

$$(Q_i,\, u_i^c,\, d_i^c,\, L_i,\, e_i^c) + (D_i,\, \bar{D}_i) + (S_i) + (H_i^u) + (H_i^d) + H' + \overline{H}', \tag{5}$$

where $i = 1,2,3$ runs over the three generations of 27_i and corresponds to the traditional three generations of matter of the SM and MSSM.

The actual Higgs fields that develop VEVs are $H_u := H_3^u$, $H_d := H_3^d$ and $S := S_3$. The remaining Higgs-like fields H_α^d, H_α^u and S_α (where $\alpha = 1, 2$ runs over the first two generations) do not develop VEVs and so are referred to as "inert" Higgs bosons.

A. The superpotential, Z_2 symmetries and soft masses

The full superpotential that can arise from the $27_i \times 27_j \times 27_k$ interactions may be written as

$$W_{E6} = W_0 + W_1 + W_2, \tag{6}$$

where

$$\begin{aligned} W_0 &= \lambda_{ijk} S_i H_j^d H_k^u + \kappa_{ijk} S_i D_j \bar{D}_k + h_{ijk}^N N_i^c H_j^u L_k \\ &\quad + h_{ijk}^U u_i^c H_j^u Q_k + h_{ijk}^D d_i^c H_j^d Q_k + h_{ijk}^E e_i^c H_j^d L_k, \end{aligned} \tag{7}$$

$$W_1 = g_{ijk}^Q D_i Q_j Q_k + g_{ijk}^q \bar{D}_i d_j^c u_k^c, \tag{8}$$

$$W_2 = g_{ijk}^N N_i^c D_j d_k^c + g_{ijk}^E e_i^c D_j u_k^c + g_{ijk}^D Q_i L_j \bar{D}_k. \tag{9}$$

However, there are phenomenological problems with such a superpotential, since at this point lepton and baryon number violating operators that lead to rapid proton decay (an obviously undesirable feature of any model) are not forbidden and there are also terms which can lead to large flavour-changing neutral currents.

In the original formulation of the E$_6$SSM [30, 31], the solution employed is to impose two discrete symmetries. The first one is an analogue of R-parity, which is either a Z_2^L symmetry, where the superfields which are odd under this symmetry are the set, $L_i, e_i^c, N_i^c, H', \overline{H}'$, or a Z_2^B symmetry, where the set of even superfields are extended to include the exotic colored superfields D_i and $\overline{D}_i$. If one assumes the Z_2^L symmetry then the interactions in W_1 are allowed and this implies that the exotic coloured superfields are diquark in nature. If one instead assumes Z_2^B then they must be leptoquark in nature, since the interactions in W_2 are allowed.

The second discrete symmetry is Z_2^H, under which S_3, H_3^d and H_3^u are even while every other field is odd. As a consequence, any term in the superpotential that violates Z_2^H (by containing superfields adding up to a net odd value) is forbidden. However, the Z_2^H symmetry cannot be exact, since it forbids all terms that would otherwise allow for the decay of exotic quarks. Therefore in the standard approach there is an approximate Z_2^H symmetry. Although this may seem rather *ad hoc*, it is worth noting that family symmetries can lead to symmetries which operate in effectively the same way as the approximate

Z_2^H symmetry introduced for phenomenological reasons [70]. Alternatively, an exact custodial symmetry may be used [36].

The couplings $\lambda_{ijk}S_iH_j^dH_k^u$, which were highlighted in the introduction (Eq. 1), are affected by this symmetry. The following couplings are suppressed by this symmetry:

$$x_{d\alpha} := \lambda_{33\alpha}, \quad x_{u\alpha} := \lambda_{3\alpha 3}, \quad z_\alpha := \lambda_{\alpha 33}, \quad c_{\alpha\beta\gamma} := \lambda_{\alpha\beta\gamma}, \tag{10}$$

where $\alpha, \beta, \gamma \in 1, 2$ runs over the inert generations of the Higgs-like states. This leaves just

$$\lambda := \lambda_{333}, \quad \lambda_{\alpha\beta} := \lambda_{3\alpha\beta}, \quad f^d_{\alpha\beta} := \lambda_{\alpha 3\beta} \quad f^u_{\alpha\beta} := \lambda_{\alpha\beta 3} \tag{11}$$

as unsuppressed couplings.

However, in order to ensure that only the third generation Higgs-like fields acquire VEVs, large Yukawa couplings should not appear in renormalization group equations (RGEs) for the soft masses of the first two generations of Higgs-like fields. As a result the f^u and f^d couplings cannot be so large and this implies that the singlinos are then always very light states since they get their masses from these interactions when H_u and H_d get VEVs.

This means that the inert-singlinos are always the lightest neutralino states. It is possible that these inert states can explain all of the observed dark matter [62]. However, constraints from direct detection of dark matter now pose a significant problem for these scenarios. In addition, in order to avoid having a cold dark matter density that is too large, such scenarios imply that the lightest Higgs decays predominantly into inert neutralinos [44], which is now ruled out by measurements of the Higgs couplings.

A solution to this was already proposed in [68], initially motivated by trying to have a relic density compatible with the cE$_6$SSM, where the f^u and f^d couplings vanish. To do this one can use an exact Z_2^S under which only the two inert-singlets, S_α, are odd. The inert-singlinos are then massless and eventually contribute only a small amount to the effective number of neutrinos. The dark matter candidate is then formed from the neutralino sector which comprises of the bino, wino, Higgsinos and inert-Higgsinos. In such scenarios a bino-like dark matter candidate may fit the measured relic density via a mechanism whereby the bino scatters inelastically off SM states into heavier inert-Higgsinos. In this mechanism the Z_2^H violating parameters that mix the inert-Higgsinos with the other neutralinos play a vital role.

Thus, we actually have three discrete symmetries restricting the terms in our superpotential. Such symmetries should be derived in an elegant way from the high-scale physics. However, since there can be more than one way to do this, leading to different couplings being suppressed, we instead choose to

take a more phenomenological approach. We assume that only the Z_2^S symmetry is exact, in order to avoid the severe problems introduced by decays to light singlinos. On the other hand, not only is the Z_2^H symmetry merely approximate, but some of the couplings which it is supposed to suppress could be quite large from a phenomenological point of view. We therefore include Z_2^H parameters that affect the neutralino masses in our analysis, performing scans involving Z_2^H violating parameters for the first time.

Since the E$_6$SSM is a broken supersymmetric model, like the MSSM, it has a large number of soft masses which parameterise the many ways that supersymmetry can be broken softly. However here we will assume minimal supergravity inspired relations amongst the soft masses, which hold true at the gauge coupling unification scale where we assume there is an E_6 grand unified theory (GUT). At this GUT scale we introduce a universal soft scalar mass (m_0) which all soft scalar masses are set equal, a universal gaugino mass, $M_{1/2}$, which all soft breaking gaugino masses are set equal to and a universal trilinear, A_0 which all the soft trilinears are set equal to. These universality conditions define the constrained version of the E$_6$SSM (cE$_6$SSM).

B. Neutralino and chargino mass mixing matrices

Our dark matter candidate is the lightest neutralino, $\tilde{\chi}_1^0$, which interacts with nucleons via spin-1 Z exchange (spin-dependent), Higgs exchange (spin-independent) and squark exchange (both spin-dependent and spin-independent). It is not the lightest R-parity odd state, since there also exist massless inert-singlinos $\tilde{\sigma}$. Despite this, it is still stable and thus viable as a dark matter candidate, since it cannot decay to $\tilde{\sigma}$: the potential $\tilde{\chi}_1^0 \to \tilde{\sigma}\sigma$ decay has no kinematically viable final states with the same quantum numbers as the lightest neutralino [68]. We focus on the spin-independent component of the neutralino-hadron cross-section, since this is overwhelmingly dominant in most direct-detection experiments.

The presence of additional fields lends a certain richness to the content of the neutralino and chargino mass mixing matrices. If the Z_2^H violating couplings in the E$_6$SSM are included, the lightest neutralino may have as many as twelve contributing fields in its interacting basis; if all Z_2^H violating couplings are neglected, however, this is reduced to six, since all interactions between third and first/second generation Higgsinos are suppressed:

$$\tilde{N}_{int} = \Big(\tilde{B} \;\; \tilde{W} \;\; \tilde{H}_d^0 \;\; \tilde{H}_u^0 \Big| \, \tilde{S} \;\; \tilde{B}' \Big)^T . \tag{12}$$

For this exploration of the EZSSM parameter space, these Z_2^H violating couplings were allowed and we adhered instead to the exact Z_2^S symmetry, resulting in a basis composed of ten fields ($\tilde{S}_u$ and $\tilde{S}_d$ are

decoupled):

$$\tilde{N}_{int} = \Big(\tilde{B} \;\; \tilde{W}^3 \;\; \tilde{H}_d^0 \;\; \tilde{H}_u^0 \;\; \tilde{S}_3 \;\; \tilde{B}' \Big| \tilde{H}_{d1}^0 \;\; \tilde{H}_{d2}^0 \;\; \tilde{H}_{u1}^0 \;\; \tilde{H}_{u2}^0 \Big)^T . \tag{13}$$

This leads to the following neutralino mass mixing matrix:

$$M^N = \left(\begin{array}{cccccc|cccc} M_1 & 0 & -\frac{1}{2}g'v_d & \frac{1}{2}g'v_u & 0 & 0 & 0 & 0 & 0 & 0 \\ 0 & M_2 & \frac{1}{2}gv_d & -\frac{1}{2}gv_u & 0 & 0 & 0 & 0 & 0 & 0 \\ -\frac{1}{2}g'v_d & \frac{1}{2}gv_d & 0 & -\mu & -\frac{\lambda v_u}{\sqrt{2}} & Q_d g_1' v_d & 0 & 0 & -\frac{\lambda_{331} s}{\sqrt{2}} & -\frac{\lambda_{332} s}{\sqrt{2}} \\ \frac{1}{2}g'v_u & -\frac{1}{2}gv_u & -\mu & 0 & \frac{\lambda v_d}{\sqrt{2}} & Q_u g_1' v_u & -\frac{\lambda_{313} s}{\sqrt{2}} & -\frac{\lambda_{323} s}{\sqrt{2}} & 0 & 0 \\ 0 & 0 & -\frac{\lambda v_u}{\sqrt{2}} & -\frac{\lambda v_d}{\sqrt{2}} & 0 & Q_s g_1' s & -\frac{\lambda_{313} v_u}{\sqrt{2}} & -\frac{\lambda_{323} v_u}{\sqrt{2}} & -\frac{\lambda_{331} v_d}{\sqrt{2}} & -\frac{\lambda_{332} v_d}{\sqrt{2}} \\ 0 & 0 & Q_d g_1' v_d & Q_u g_1' v_u & Q_s g_1' s & M_1' & 0 & 0 & 0 & 0 \\ \hline 0 & 0 & 0 & -\frac{\lambda_{313} s}{\sqrt{2}} & -\frac{\lambda_{313} v_u}{\sqrt{2}} & 0 & 0 & 0 & -\frac{\lambda_{311} s}{\sqrt{2}} & -\frac{\lambda_{312} s}{\sqrt{2}} \\ 0 & 0 & 0 & -\frac{\lambda_{323} s}{\sqrt{2}} & -\frac{\lambda_{323} v_u}{\sqrt{2}} & 0 & 0 & 0 & -\frac{\lambda_{321} s}{\sqrt{2}} & -\frac{\lambda_{322} s}{\sqrt{2}} \\ 0 & 0 & -\frac{\lambda_{331} s}{\sqrt{2}} & 0 & -\frac{\lambda_{331} v_d}{\sqrt{2}} & 0 & -\frac{\lambda_{311} s}{\sqrt{2}} & -\frac{\lambda_{312} s}{\sqrt{2}} & 0 & 0 \\ 0 & 0 & -\frac{\lambda_{332} s}{\sqrt{2}} & 0 & -\frac{\lambda_{332} v_d}{\sqrt{2}} & 0 & -\frac{\lambda_{321} s}{\sqrt{2}} & -\frac{\lambda_{322} s}{\sqrt{2}} & 0 & 0 \end{array} \right) , \tag{14}$$

where $Q_d = -\frac{3}{\sqrt{40}}$, $Q_u = -\frac{2}{\sqrt{40}}$ and $Q_s = -\frac{5}{\sqrt{40}}$ are the $U(1)_N$ charges of the down-type Higgs doublets, the up-type Higgs doublets and the SM-singlets respectively. Furthermore, M_1, M_2 and M_1' are soft gaugino masses, while g_1' is the GUT normalised $U(1)_N$ gauge coupling. The top-left block of this matrix is the usual NMSSM neutralino mass mixing matrix with an additional row and column for the $U(1)$ bino - this block will be referred to as the USSM sector. The rest are contributions from couplings with the inert-Higgsinos. Note that if the approximate Z_2^H symmetry were to be enforced (by limiting $\lambda_{3\alpha 3}$ and $\lambda_{33\alpha}$ from above by imposing flavour changing neutral current (FCNC) constraints), the bottom right corner would become an approximately decoupled block diagonal mass matrix in a basis consisting of the inert-Higgsinos. For completion, we also write down the interaction basis of the chargino:

$$\tilde{C}_{int} = \Big(\tilde{W}^+ \;\; \tilde{H}_{u3}^+ \Big| \tilde{H}_{u2}^+ \;\; \tilde{H}_{u1}^+ \Big| \tilde{W}^- \;\; \tilde{H}_{d3}^- \Big| \tilde{H}_{d2}^- \;\; \tilde{H}_{d1}^- \Big)^T . \tag{15}$$

The chargino mass mixing matrix is:

$$M^C = \begin{pmatrix} 0 & P^T \\ P & 0 \end{pmatrix} , \tag{16}$$

where

$$P = \left(\begin{array}{cc|cc} M_2 & \sqrt{2}m_W s_\beta & 0 & 0 \\ \sqrt{2}m_W c_\beta & \mu & \frac{1}{\sqrt{2}}\lambda_{332}s & \frac{1}{\sqrt{2}}\lambda_{331}s \\ \hline 0 & \frac{1}{\sqrt{2}}\lambda_{323}s & \frac{1}{2}\lambda_{322}s & \frac{1}{\sqrt{2}}\lambda_{321}s \\ 0 & \frac{1}{\sqrt{2}}\lambda_{313}s & \frac{1}{\sqrt{2}}\lambda_{312}s & \frac{1}{\sqrt{2}}\lambda_{311}s \end{array}\right). \tag{17}$$

III. SCAN PROCEDURE

Following the considerations in the previous section, we perform a scan over x_{u1}, x_{d1}, x_{u2}, x_{d2}, λ_{11}, $\tan\beta$, λ, λ_{22}, s and κ, where x_{u1} and x_{u2} are the $SH_{dj}H_{u3}$ couplings with $j = 1, 2$, x_{d1} and x_{d2} are the $SH_{d3}H_{uk}$ couplings with $k = 1, 2$, and finally λ_{mn} are the $SH_{dm}H_{un}$ couplings with $m, n = 1, 2$. We do not scan over the universal soft masses as these are output parameters determined by the spectrum generator in our setup, as will be explained shortly.

The large dimensionality of this parameter set makes a random or grid scanning method prohibitively expensive. For efficient sampling we use `Multinest-2.4.5` which employs a nested sampling algorithm to calculate the Bayesian evidence of the model by Monte Carlo integration, obtaining posterior samples as a by-product [71–73].

However in this study we do not consider the Bayesian evidence or the posterior samples. Instead, we simply use `Multinest` as a tool to quickly find E_6SSM parameters that give rise to the observed relic abundance of dark matter whilst remaining consistent with the LHC Higgs mass measurement, and have a WIMP-nucleon cross-section for the lightest neutralino that lies close to the current experimental exclusion limits. To do this, we passed the following 'likelihood' function to Multinest:

$$\log L = -\left(\frac{m_{h_1} - m_{h_1}^{\rm ex}}{\sigma^{m_{h_1}}}\right)^2 - \left(\frac{\Omega h^2 - (\Omega h^2)^{\rm obs}}{\sigma^{\Omega h^2}}\right)^2 - \left(\frac{\sigma_{\rm SI} - \sigma_{\rm SI}^{\rm lim}}{0.5\sigma_{\rm SI}^{\rm lim}}\right)^2. \tag{18}$$

Note that the density of points in our final plots will not have a clear meaning, and we will instead only focus on the type of dark matter solution that we encounter.

The first term is the constraint from the LHC Higgs mass measurement, where we use the 2012 CMS result $m_h^{\rm ex} = 125.3$ GeV with $\sigma^{m_{h_1}} = 0.64$ GeV, consisting of a quadrature sum of the quoted systematic and statistical errors [74]. This has since been improved to $m_h^{\rm ex} = 125.09$ GeV with $\sigma^{m_{h_1}} = 0.24$ GeV by combined CMS and ATLAS measurements [75], but the details will not affect our final conclusions. The second term is the constraint from the relic density, assuming a central value of $(\Omega h^2)^{\rm obs} = 0.1196$. This is using the 2013 value from the Planck collaboration along with associated uncertainty $\sigma^{\Omega h^2} = 0.0031$[76]. The third and final term is the constraint on the WIMP-nucleon SI cross-section from the 2013 LUX results [63]. Here, the function $\sigma_{\rm SI}^{\rm lim}$ was extrapolated from the 95% confidence level LUX limit, and

the final term ensures that we find solutions close to the current experimental reach. The LUX results have been updated recently [65] imposing substantially stronger limits on the spin-independent cross-section. Nonetheless we also compare our final results from the scan with these recent LUX results which appeared after the scan had completed. The large width of the Gaussian function used above is sufficient to give us solutions that are beyond the current LUX reach, however, and we briefly comment on the impact in the next section. We assume a flat prior on all parameters, and scan within the ranges given in Table I.

Parameter	Range	Parameter	Range
x_{u1}	$0 - 0.5$	x_{u2}	$0 - 0.5$
x_{d1}	$0 - 0.5$	x_{d2}	$0 - 0.5$
λ_{11}	$0.0001 - 1.0$	λ_{22}	$0.0001 - 1.0$
$\tan\beta$	1 - 40	s	$0 - 100000$
λ	$-0.5 - 0.5$	κ	$0 - 5$

TABLE I. The parameters used in our scan, along with the allowed ranges.

For each point in our scan, we calculate the mass spectrum using an unpublished spectrum generator that uses semi-analytic solutions for the soft masses as described in Refs.[46, 47]. The semi-analytic solutions express the soft masses, including those appearing in the electroweak symmetry breaking conditions, in terms of the universal soft masses, m_0, $M_{1/2}$ and A_0 which are fixed at the GUT scale. As a result the universal softmasses can be parameters which are fixed by the electroweak symmetry breaking conditions. Without this procedure it is hard to solve the constrained version of the model, as one wants to fufill the EWSB constraint by fixing a softmass at the electroweak scale, while also requiring it fulfills the high scale universality condition. We run all soft masses, superpotential parameters and gauge couplings between the electroweak and GUT scale with the full two-loop RGEs, by linking to `FlexibleSUSY` [77, 78], which uses `SARAH` [79–83] and numerical routines from `SOFTSUSY` [84, 85]. The Higgs mass is calculated by generalising an NMSSM calculation using EFT techniques but expanded to fixed two-loop order, as described in [30, 47]. Since we expect at the outset to have a very heavy SUSY scale and also allow exotic couplings in the scan to be large, using the full two-loop fixed order calculation for this model [1] or an MSSM effective field theory computation [2] would not significantly improve the precision, while an E_6SSM effective field theory computation was not available when this work was performed [3]. We do not expect our results to be substantially changed by a more accurate determination of the Higgs mass. The relic density of dark matter and WIMP-nucleon cross-section for the lightest neutralino are obtained using a version of `micrOMEGAs-2.4.5` [88–90], which was extended[4]

[1] Recently this has been made possible with `SARAH` / `SPheno` [86].
[2] As was done in Ref.[67] using `SUSYHD`[87].
[3] Such a calculation [91] was made available while this paper was being finalised.
[4] We thank Jonathan Hall for supplying us with this version of `micrOMEGAs`.

for the E_6SSM with an E_6SSM `CalcHEP` [92] model file generated using `LanHEP` [93].

As well as using the measured Higgs mass, dark matter relic density and LUX limits to guide the scan we also apply explicit experimental constraints to the data before plotting results. Unless explicitly stated otherwise we require that each point fulfills the following:

$$(\Omega h^2)^{\rm obs} - 2\sigma^{\Omega h^2} > \Omega h^2 > (\Omega h^2)^{\rm obs} + 2\sigma^{\Omega h^2} \tag{19}$$

$$122.3\,{\rm GeV} < m_h < 128.3\,{\rm GeV} \tag{20}$$

$$m_{\rm gluino} > 1.4\,{\rm TeV} \tag{21}$$

$$M_{Z'} > 2.85\,{\rm TeV} \tag{22}$$

$$\mu_{D_i} > 1.4\,{\rm TeV} \tag{23}$$

$$m_{\chi_i^\pm} > 100\,{\rm GeV} \tag{24}$$

Here we give a large 6 GeV range for the Higgs mass, m_h to account for the well known large theoretical errors associated with this prediction. Since the scan was designed to efficiently find points with a Higgs mass prediction close to the experimentally measured value this does not cut out many points. The constraint on the relic density ensures that we can explain all of the dark matter relic abundance, while not over closing the universe. Since the focus of our work is the direct detection phenomenology of the E_6SSM, we do not include collider constraints in our scan. However, as has been discussed previously [49], the hierarchical spectrum in the constrained E_6SSM means that sfermions will be safe from LHC limits so long as the gluino is above the CMSSM limit in the heavy sparticle limit, which is what we impose here[5]. We also require that the exotic coloured fermions, which could potentially be light, have a mass, μ_{D_i}, greater than 1.4 TeV, since we expect the signature to be comparable to that of the gluinos, though no dedicated quantitative analysis has been done for these states. At the same time, LEP limits on charginos should be rather robust and we use these to set a lower limit on the lightest chargino states in this model. Finally we use the latest Z' limits to ensure that this would not have been discovered as a peak in the dilepton invariant mass spectrum at the LHC.

IV. RESULTS AND DISCUSSION

A. Dark Matter candidates and their spin-independent cross-section

We now turn to a discussion of the results of our scan, including the possible dark matter explanations that have been revealed and the implications for these from dark matter direct detection experiments.

[5] In cases where there are additional light neutralinos compared to the MSSM the gluino cascade decay can be modified, which can alter the gluino mass limit [94, 95]. However this would not have a large impact on our results.

The spin-independent cross-section (σ_{SI}) for direct detection of dark matter is shown in Figure 1 for all points which pass our experimental constraints given in Eqs. 19–24. In the left panel σ_{SI} is shown as a colour contour in the $m_0 - M_{1/2}$ plane. Care should be taken when interpreting this plot as the very different renormalisation group flow of the E$_6$SSM, compared to the MSSM, means that the relationship between soft masses at low energies (and thereby the physical mass eigenstates) and universal soft masses at the GUT scale is changed considerably. The right panel shows σ_{SI} plotted directly against the neutralino mass, with the minimum gluino mass from each bin plotted as a colour contour.

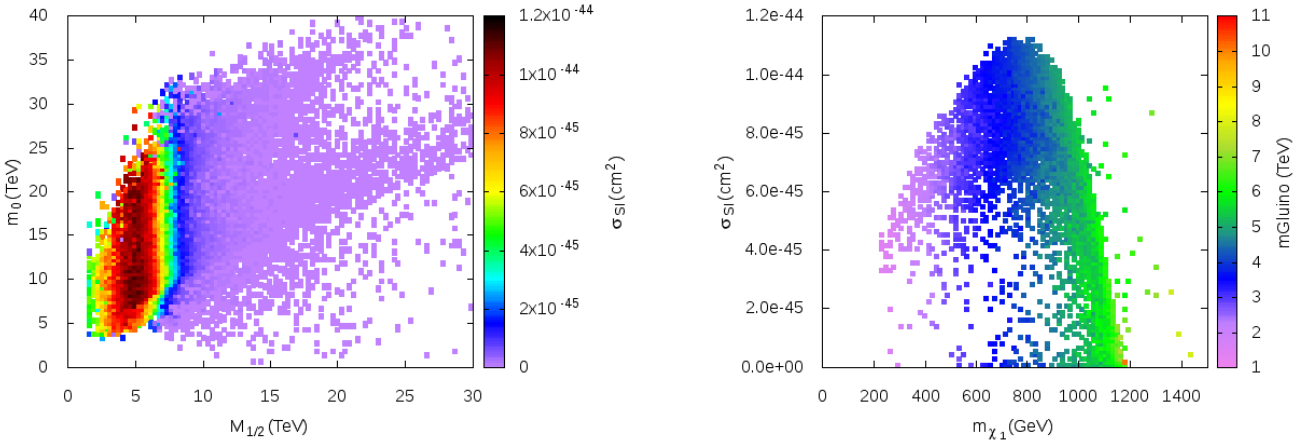

FIG. 1. The spin-independent cross-section for direct detection of dark matter for all points found in the scan consistent with Eqs. 19–24. Left panel: the $m_0 - M_{1/2}$ plane with the maximum binned value of σ_{SI} given as the colour contour. Right panel: σ_{SI} against the lightest neutralino mass, m_{χ_1}. A colour contour of the lightest gluino mass in each bin is shown to indicate in which cases gluino production could be observed at the LHC.

The left panel shows that we can explain the full relic abundance of dark matter, while satisfying collider constraints, for much of the $m_0 - M_{1/2}$ plane. Comparing this to the right panel we see that this happens for dark matter candidates with a wide range of masses, though the density of solutions found varies a lot. The correct relic density is achieved through several different mechanisms, which depend on the nature of the dark matter candidate. In this model the dark matter candidate is the lightest neutralino, which may be bino-like, Higgsino-like, inert-Higgsino-like or some combination of two or all three of these; we will discuss each case briefly.

As can be seen in the left panel many solutions we have found go way beyond the reach of the LHC. While the heavy SUSY scale there makes it very challenging to predict the Higgs mass precisely we expect that our result here should be reproducible with higher precision calculations that have been recently developed [91], requiring only adjustments to parameters that are essentially orthogonal to the other predictions we present. When $M_{1/2} \gtrsim 8$ TeV this implies that M_1 is significantly larger than ≈ 1 TeV and the correct relic density can be explained without a large bino component to the dark matter.

As the colour contour in the right panel of Figure 1 shows, the large $M_{1/2}$ values required for these points means that the gluino is very heavy and well beyond the reach of the LHC. In this case the dark matter candidate is either pure Higgsino, pure inert-Higgsino or a mixture of the two and these solutions are found in the dense almost vertical band of solutions shown in the lower right region of the right panel of Figure 1.

This is confirmed in Figure 2 where in the left panel the bino content is shown varying across the $m_{\chi_1^0} - \sigma_{SI}$ plane. The Higgsino and inert-Higgsino dark matter candidates both obtain the correct relic density through the same annihilation mechanisms as Higgsino dark matter in the MSSM, which is why these scenarios have a mass of around 1 TeV.

For dark matter candidates with no bino content (defined here as having less than 10% bino component) the standard co-annihilation mechanism does not allow the correct relic density to be obtained outside of this band. When such a dark matter candidate is lighter than this it will typically give a relic density which is too large as a light Higgsino annihilates too efficiently, as can be seen in the right panel of Figure 2. Similarly if the mass is larger than the masses in this band then the dark matter will not annihilate enough leading to over-closure of the universe.

This prediction can be evaded if there is a non-standard mechanism for Higgsino dark matter, such as a funnel region. Indeed the small number of scattered Higgsino or inert-Higgsino points that still fit the relic density very well, while having $m_{\chi_1^0} > 1.2$ TeV, correspond to A-funnel scenarios where the pseudoscalar Higgs mass is very close to being twice the mass of the lightest neutralino.

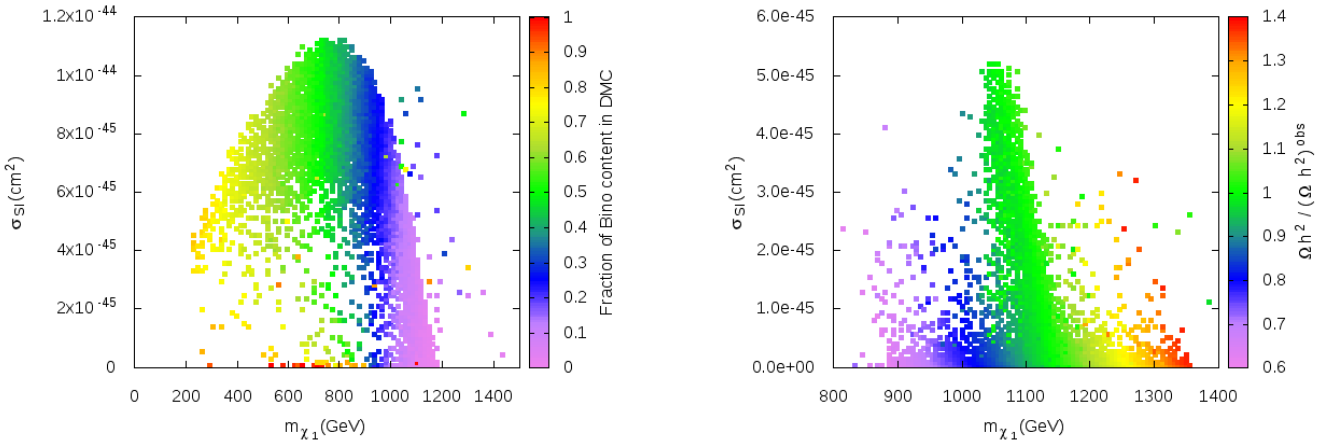

FIG. 2. Spin-independent cross-section, σ_{SI}, against the lightest neutralino mass, m_{χ_1}. In the left panel we show the bino content of the dark matter as a colour contour and plots all points found in the scan that satisfy the experimental constraints in Eqs. 19–24. The right panel shows a colour contour of the minimum value of $\Omega h^2/(\Omega h^2)^{obs}$, in each bin for points with less than 10% bino content that satisfy all constraints in Eq. 20–24, omitting only the condition on the relic density so that the variation can be shown.

Another possibility is that the neutralino is predominantly bino. Pure bino scenarios have very low spin-independent direct detection cross-sections, as the SM-like Higgs exchange diagram is suppressed. However in the MSSM, the current mass limits on sparticles make it quite difficult to successfully achieve the correct relic density for a pure bino. In contrast in the cEZSSM there is a special mechanism which can achieve the correct relic density with a predominantly bino-like dark matter candidate that was proposed in Ref. [68]. There the relic density is achieved in a manner which is not possible in the MSSM, involving scattering off of standard model states into inert-Higgsinos, which must not be much heavier than the bino.

In addition we also find scenarios where the dark matter candidate is pure bino and the mass is around half that of the pseudoscalar Higgs boson. This gives us the bino A-funnel scenario, where, as in the MSSM, this tuning allows the annihilation cross-section to be large enough that the pure bino candidate does not over-close the universe.

Another possibility to obtain the measured relic density with a lightest neutralino mass lower than $\approx$ 1 TeV, away from this Higgsino/inert-Higgsino band, is to tune the parameters to lie in the well-tempered region [96]. As in the CMSSM the wino is always heavier than the bino, so such scenarios will have a significant admixture of bino and inert-Higgsino or Higgsino dark matter, as can be seen in the left panel of Figure 2. While scenarios where the dark matter candidate is predominantly composed of just one gauge eigenstate have a suppressed spin-independent cross-section (and in the case of Higgsinos and inert-Higgsinos a very heavy mass spectrum), scenarios with mixed dark matter candidates can be quite different.

In particular, it is well known that in the MSSM one may also obtain the correct relic density for mixed bino-Higgsino candidates [96]. This scenario avoids requiring M_1 to be significantly greater than $m_{\chi_1^0} \approx 1$ TeV, and therefore gives rise to better prospects for discovery in collider experiments. However, introducing more bino-Higgsino mixing enhances the direct search cross-section by increasing the contribution from Higgs exchange, as can be seen in the top left panel of Figure 3, where we plot σ_{SI} as a colour contour with the Higgsino, and bino content as the axes. This has already been discussed in Ref. [67] for constrained versions of the MSSM and an alternative E_6-inspired model, where it was shown that the bino-Higgsino mixing is now heavily constrained by LUX [63–65].

However, unlike the E_6-inspired models considered in Refs.[66, 67], in the cEZSSM there are further possibilities involving the inert-Higgsinos. Since associated inert-Higgs bosons are all very heavy, the s-channel annihilation diagram involving the inert-Higgs is suppressed and in this case the correct relic density is simply obtained by diluting the inert-Higgsino co-annihilation mechanism through the reduced inert-Higgsino content. The heavy inert-Higgs states also mean that the direct detection cross-section is suppressed as is shown in the top right panel of Figure 3, so the inert-Higgsinos mixing with the

bino does not lead to large spin-independent cross-sections. There is no bino-Higgs-inert-Higgsino for a SM-like Higgs exchange contribution and the inert-Higgs scalar is very heavy, which suppresses an inert-Higgs exchange contribution to the cross-section. Note that these plots include scenarios where the dark matter candidate contains significant admixtures of all three types (Higgsino, inert-Higgsino and bino) of gauge states. This is why the cross-section can become large here as well for moderate values of the bino and inert-Higgsino contents, where they do not sum to unity.

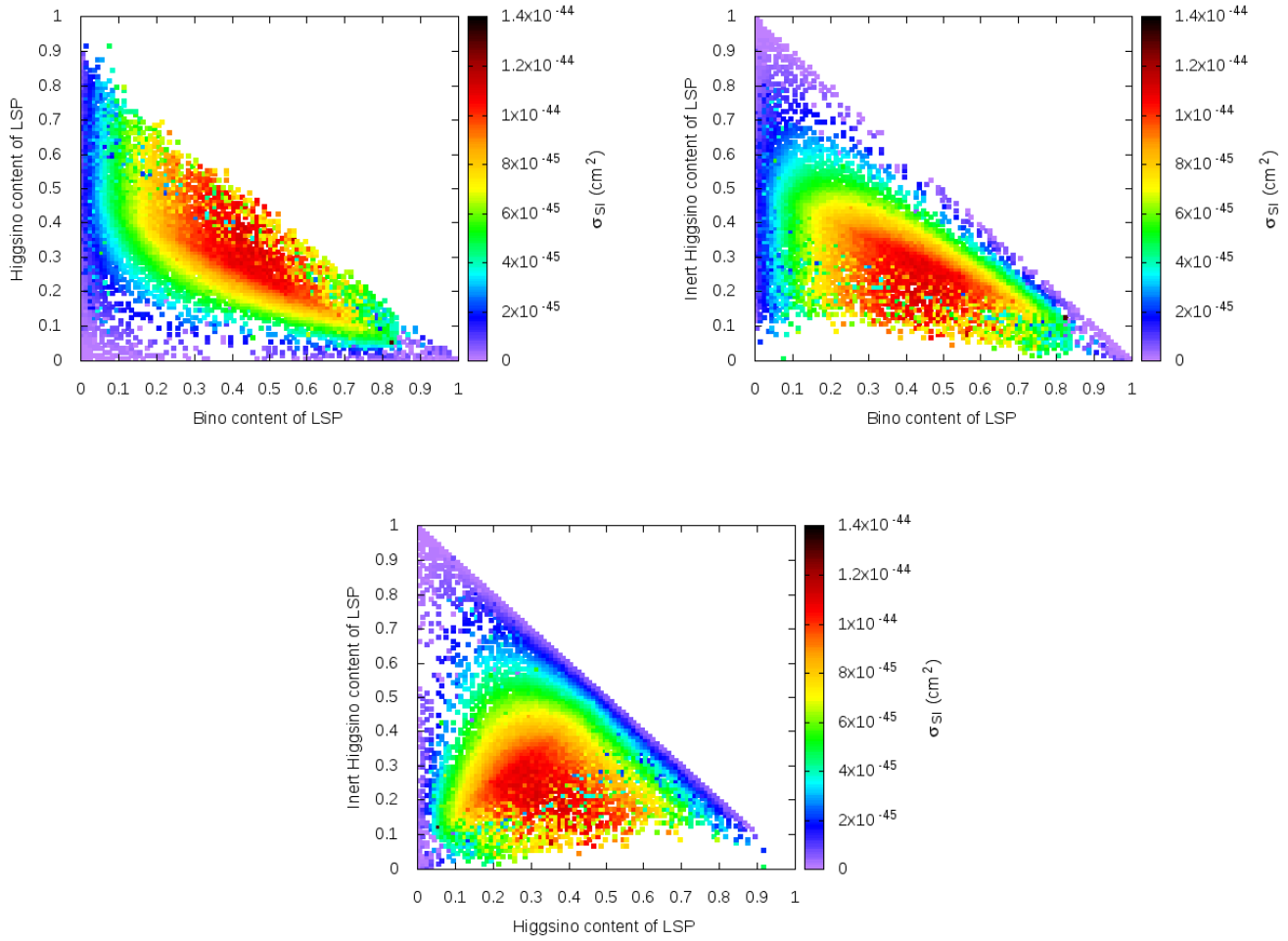

FIG. 3. Spin-independent cross-section, σ_{SI}, varying with the content of the lightest neutralino. To illustrate the mechanism clearly, we do not impose any experimental constraints in these plots. In the top left panel we plot σ_{SI} as a colour contour with the bino content on the x-axis and the Higgsino content on the y-axis. In the top right panel we show the same, but with the inert-Higgsino content on the y-axis instead of the Higgsino content. In the bottom panel we have Higgsino content on the x-axis and inert-Higgsino content on the y-axis.

B. Impact of direct detection experiments

Applying the LUX 2015 and LUX 2016 constraints to our results, as shown in Figure 4 demonstrates the dramatic impact of LUX 2016, ruling out many scenarios. As one could anticipate the pure Higgsino/inert-Higgsino scenarios can survive, and these correspond to the large region of $m_0 - M_{1/2}$ parameter space at larger $M_{1/2}$ where the spin-independent cross-section is rather small. Note that in this case the limit on $M_{1/2}$ for Higgsino dark matter set by the LUX experiment exceeds the LHC reach considerably. However scenarios with a sub-TeV dark matter candidate can be more relevant to collider phenomenology.

Since the scan was designed to find scenarios close to the direct detection cross-sections limits of LUX 2013, it is not surprising that so many scenarios we found are now ruled out. Nonetheless the results have still revealed the possibility of mixed bino inert-Higgsino dark matter, and in these cases the cross-section can be considerably weaker, while still fitting the relic density.

While only a small number of these points lying below the LUX 2016 limit were found, they do provide a novel way to escape the stringent limits from the latest direct detection experiments.

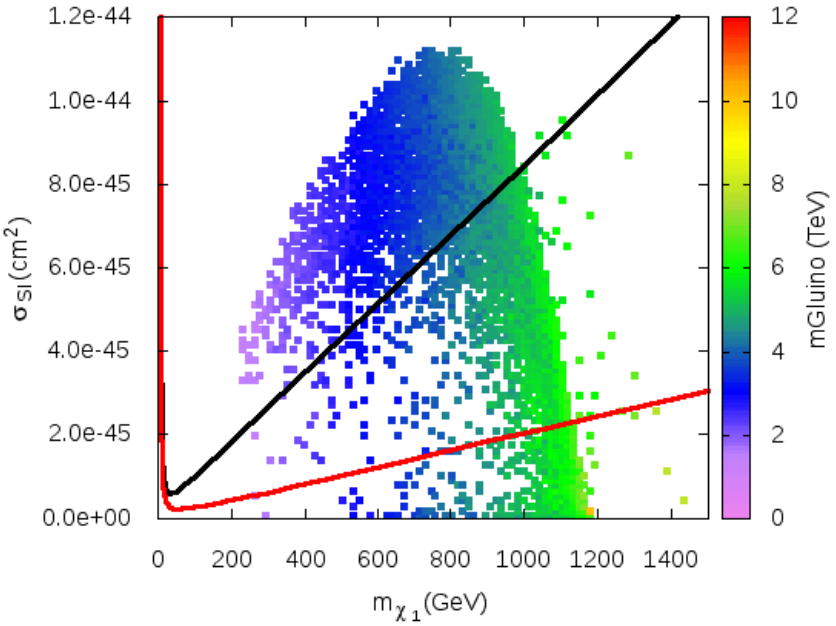

FIG. 4. Spin-independent cross-section, σ_{SI}, against the lightest neutralino mass, m_{χ_1} with the minimum gluino mass in each bin plotted as a colour contour. All experimental constraints from Eqs.19–24 are applied. The black curve shows the LUX 2015 limit [64], while the LUX 2016 limit [65] is indicated by the red curve.

To illustrate the scenarios which can evade the LUX limits we present five benchmark scenarios in Table II. These benchmark scenarios represent the different mechanisms we found where the relic density

can be fitted while still evading the LUX limits. These possibilities are as follows.

First the dark matter may simply be composed of only Higgsino or inert-Higgsino gauge states. Higgsino dark matter is a well known possibility in the MSSM and has also been studied in other E_6-inspired scenarios that have been explored previously [67]. BM1 is a scenario where the dark matter relic density is explained from a neutralino dark matter candidate that is predominantly inert-Higgsino in nature. The dominant channels in this case, are chargino-neutralino co-annihilations, as is the case for standard Higgsino dark matter. Since this inert-Higgsino dark matter candidate has a mass of 1.1 TeV, the observed relic density can be fitted, while the spin-independent cross-section is sufficiently small that the LUX limits can be evaded.

Typically if a pure Higgsino or inert-Higgs dark matter candidate has a mass much lower than that of BM1 the predicted relic density will be too small, while if the mass is much higher then it will be too large, leading to over-closure of the universe. However the latter can be avoided if these annihilations are enhanced by a funnel mechanism. BM2 shows a Higgsino dark matter candidate where the pseudoscalar Higgs boson has a mass, $m_{A^0} \approx 2m_{\chi_1^0}$, allowing the observed relic density to be achieved predominantly through near-resonant annihilation through the pseudoscalar Higgs boson into $b\bar{b}$. Such scenarios are commonly referred to as A-funnel scenarios in the literature.

For lighter dark matter, one may consider special bino dark matter scenarios. BM3 shows a dark matter candidate which is made up primarily of the bino gauge eigenstate. The relic density for these scenarios is satisfied through the mechanism previously explored in Ref. [68], which requires that there is a predominantly inert-Higgsino neutralino with a mass very close to the lightest neutralino. This mechanism proceeds by the lightest neutralino up-scattering into the slightly heavier inert-Higgsino neutralino, which then co-annihilates at a rate large enough to fit the observed relic density. BM4 shows another possibility where the bino-like dark matter candidate annihilates through the pseudoscalar Higgs boson into mostly $b\bar{b}$, giving another A-funnel possibility, a type of scenario that is well known in the MSSM and has also been looked at in E_6-inspired models previously [67].

Finally BM5 shows a new possibility that has not been discussed previously in the literature. In this scenario the dark matter candidate has large admixtures of bino and inert-Higgsino. While scenarios where the bino mixes only with a Higgsino are heavily constrained due to the large spin-independent cross-section obtained through Higgs exchange, these scenarios are free of this problem since there is no light inert-Higgs state to give rise to a large inert-Higgs exchange contribution to the spin-independent cross-section. Similarly unlike standard cases of a mixed Higgsino-bino candidate where the relic density is achieved by annihilation mostly through the light Higgs boson[6], in this case the observed relic density is achieved only through the usual co-annihilation channels of Higgsino dark matter. Over-closure of

[6] See for example benchmarks given in Ref. [66].

the universe is avoided because of the bino mixing, which dilutes the efficiency of this process.

C. Conclusions and Outlook

We have presented the most extensive phenomenological exploration of the cE$_6$SSM to date, and revealed a large volume of parameter space compatible with the measured relic abundance of dark matter and the latest results from the LHC, including a 125 GeV Higgs boson and collider limits on new states. This work has revealed a number of different scenarios for explaining the observed relic density of dark matter. We have shown the significant impact of the recent direct detection limits. However even with these tough limits there are a number of mechanisms for obtaining the measured relic density that can have a spin-independent direct detection cross-section below the LUX 2016 limit.

In particular if the dark matter candidate is a mixture of inert-Higgsino and bino it can be significantly lighter than 1 TeV and still predict the correct relic density and evade the LUX 2016 limit for direct detection. Another possibility in this model is a pure bino dark matter candidate, where the relic density can be obtained either through an up-scattering into inert-Higgsinos which then co-annihilate with charged inert-Higgsinos, or through A-funnel scenarios. Such scenarios are more likely to be observed in the last part of LHC Run II, or during subsequent runs at high luminosity. Certainly they have much better prospects for observability in collider experiments than the pure Higgsino or inert-Higgsino scenarios, where the gluino must be heavier than about 6 TeV.

Nonetheless even the pure Higgsino and inert-Higgsino scenarios which we explored here will be within range of XENON1T [97]. The XENON1T experiment is the third phase of the XENON experiment at the Gran Sasso Laboratory and will soon begin to publish results. The sensitivity of this experiment is expected to reach a minimum spin-independent WIMP-nucleon cross-section of 1.6×10^{-47} cm^2 at $m_\chi = 50$ GeV, a factor of approximately 50 times better than the current LUX limit at the same WIMP mass [97]. This is sensitive enough to be able detect all of the benchmark points we have presented and will provide severe constraints on the model.

ACKNOWLEDGEMENTS

We gratefully acknowledge the help of Jonathan Hall in providing the modified `micrOMEGAs` program with the E6SSM model file and spectrum generator embedded. PA would like also like to thank Steve King for early discussions about the viability of this project, Roman Nevzorov for very illuminating discussions about possible dark matter candidates in E_6-inspired models and Andrew Fowlie for reading through a draft of the manuscript and providing useful feedback. This work was supported by the

	BM1	**BM2**	**BM3**	**BM4**	**BM5**
λ	-0.0655	0.18122	-0.552579	0.0831877	0.285842
κ	0.2211	0.169603	0.22825	0.122173	0.230147
$\tan\beta$	29.3	22.4239	5.4816	38.5743	7.1522
s (GeV)	52966.4	70523.5	16739.2	29474.3	73442.8
λ_{11}	0.2435763862	0.316856	0.048464	0.0903254	0.617126
λ_{22}	0.02779747502	0.654349	0.588343	0.795588	0.0171
x_{u1}	0.1196894578	0.271995	0.0626005	0.0344383	0.167725
x_{d1}	0.3668858675	0.169106	0.062843	0.464061	0.0910559
x_{u2}	0.01118730707	0.0093813	0.434091	0.0691506	0.0179128
x_{d2}	0.08349296723	0.439901	0.351041	0.270508	0.0641696
m_0 (GeV)	19262.0	26562.8	4069.08	13741.2	19330.3
$M_{1/2}$ (GeV)	7387.5	9492.72	4008.4	3467.43	3338.41
A_0	6269.1	16767.1	-574.161	10650.9	24157.8
Ωh^2	0.1190	0.1162	0.1180	0.1240	0.1223
σ_{SI} (cm^2)	1.20×10^{-46}	1.106×10^{-46}	1.60×10^{-47}	2.86×10^{-45}	4.53×10^{-46}
$m_{\tilde{\chi}_1^0}$ (GeV)	1104.0	1387.9	631.3	557.1	543.7
$m_{\tilde{\chi}_2^0}$ (GeV)	1106.0	1393.9	643.0	656.8	563.3
$m_{\tilde{\chi}_3^0}$ (GeV)	1167.9	1521.8	643.8	658.3	567.3
$m_{\tilde{\chi}_4^0}$ (GeV)	2069.4	2700.2	1118.8	1023.5	980.9
$m_{\tilde{\chi}_5^0}$ (GeV)	5300.8	21956.5	5621.4	9152.0	10496.1
$m_{\tilde{\chi}_1^\pm}$ (GeV)	1105.7	1392.3	642.9	648.9	562.5
$m_{\tilde{\chi}_2^\pm}$ (GeV)	2069.4	2700.2	643.0	1023.4	980.9
$m_{\tilde{\chi}_3^\pm}$ (GeV)	5301.5	21956.6	5622.7	9152.0	10496.3
m_{h_1} (GeV)	124.8	125.4	122.7	125.0	127.2
m_{A^0} (GeV)	11900	2838.6	6329.1	1093	9393
$m_{\tilde{t}_1}$(GeV)	15200	19600	4920	9290	13300
$m_{Z'}$ (GeV)	19600	26100	6190	10905	27200
$\lvert Z(N)_{11}\rvert^2$	0.0238	0.0292	0.924	0.901	0.788
$\lvert Z(N)_{12}\rvert^2$	0.0003	0.000989	1.06×10^{-5}	0.00125	0.000354
$\lvert Z(N)_{13}\rvert^2$	6.46×10^{-6}	0.292	0.0001522	0.00211	0.00144
$\lvert Z(N)_{14}\rvert^2$	0.0497	0.289	0.0003186	0.0407	0.00961
$\lvert Z(N)_{15}\rvert^2$	1.72×10^{-7}	6.41×10^{-7}	7.03×10^{-9}	4.61×10^{-7}	1.43×10^{-8}
$\lvert Z(N)_{16}\rvert^2$	1.36×10^{-9}	3.96×10^{-7}	1.15×10^{-8}	7.27×10^{-9}	7.21×10^{-11}
$\lvert Z(N)_{17}\rvert^2$	0.4886	0.132	7.50×10^{-5}	0.000226	0.108
$\lvert Z(N)_{18}\rvert^2$	0.4250	6.12×10^{-5}	0.000196	0.000290	0.0921
$\lvert Z(N)_{19}\rvert^2$	9.80×10^{-5}	0.0624	0.0383	0.0546	3.60×10^{-5}
$\lvert Z(N)_{110}\rvert^2$	0.0123	0.193	0.0370	5.91×10^{-5}	0.000713

TABLE II. The five benchmark points chosen in this study. **BM1** features a lightest neutralino with a high inert-Higgsino content. **BM2** features a lightest neutralino that is a mixture of Higgsino and inert-Higgsino. The lightest neutralino of **BM3** has a pure-bino character and the model satisfies the relic density constraint through the upscattering mechanism. **BM4** also has a pure-bino LSP, and in this case the model achieves the correct relic density through resonant annihilation via the A boson. Finally, **BM5** has an LSP with a mixture of bino and inert-Higgsino components.

University of Adelaide, Monash University and the Australian Research Council through the ARC

	BM1	BM2	BM3	BM4	BM5
$\tilde{\chi}_1^0\tilde{\chi}_1^+ \to t\bar{b}$	7.2%	12%	4%	<1%	5%
$\tilde{\chi}_1^0\tilde{\chi}_1^+ \to u\bar{d}$	7.0%	5%	4%	<1%	5%
$\tilde{\chi}_1^0\tilde{\chi}_1^+ \to c\bar{s}$	6.9%	5%	4%	<1%	5%
$\tilde{\chi}_1^0\tilde{\chi}_1^+ \to n_1\bar{e}_1$	2.4%	2%	1%	<1%	2%
$\tilde{\chi}_1^0\tilde{\chi}_1^+ \to n_2\bar{e}_2$	2.4%	2%	1%	<1%	2%
$\tilde{\chi}_1^0\tilde{\chi}_1^+ \to n_3\bar{e}_3$	2.4%	2%	1%	<1%	2%
$\tilde{\chi}_1^0\tilde{\chi}_1^+ \to ZW^+$	1.0%	<1%	<1%	<1%	<1%
$\tilde{\chi}_1^0\tilde{\chi}_1^+ \to AW^+$	1.2%	<1%	<1%	<1%	<1%
$\tilde{\chi}_1^0\tilde{\chi}_1^+ \to h_1W^+$	0.6%	<1%	<1%	<1%	<1%
$\tilde{\chi}_2^0\tilde{\chi}_1^+ \to t\bar{b}$	6.1%	4%	5%	<1%	5%
$\tilde{\chi}_2^0\tilde{\chi}_1^+ \to u\bar{d}$	5.9%	3%	5%	<1%	5%
$\tilde{\chi}_2^0\tilde{\chi}_1^+ \to c\bar{s}$	6.9%	3%	5%	<1%	5%
$\tilde{\chi}_3^0\tilde{\chi}_1^+ \to t\bar{b}$	<1%	<1%	4%	<1%	3%
$\tilde{\chi}_3^0\tilde{\chi}_1^+ \to u\bar{d}$	<1%	<1%	4%	<1%	3%
$\tilde{\chi}_3^0\tilde{\chi}_1^+ \to c\bar{s}$	<1%	<1%	4%	<1%	3%
$\tilde{\chi}_2^0\tilde{\chi}_1^+ \to n_1\bar{e}_1$	2.1%	1%	2%	<1%	2%
$\tilde{\chi}_2^0\tilde{\chi}_1^+ \to n_2\bar{e}_2$	2.1%	1%	2%	<1%	2%
$\tilde{\chi}_2^0\tilde{\chi}_1^+ \to n_3\bar{e}_3$	2.1%	1%	2%	<1%	2%
$\tilde{\chi}_3^0\tilde{\chi}_1^+ \to n_1\bar{e}_1$	<1%	<1%	1%	<1%	1%
$\tilde{\chi}_3^0\tilde{\chi}_1^+ \to n_2\bar{e}_2$	<1%	<1%	1%	<1%	1%
$\tilde{\chi}_3^0\tilde{\chi}_1^+ \to n_3\bar{e}_3$	<1%	<1%	1%	<1%	1%
$\tilde{\chi}_1^0\tilde{\chi}_1^0 \to W^+W^-$	1.8%	2%	1%	<1%	2%
$\tilde{\chi}_1^0\tilde{\chi}_3^0 \to W^+W^-$	<1%	<1%	1%	<1%	<1%
$\tilde{\chi}_1^0\tilde{\chi}_1^0 \to ZZ$	1.5%	1%	<1%	<1%	2%
$\tilde{\chi}_1^0\tilde{\chi}_1^0 \to t\bar{t}$	0.0%	<1%	<1%	12%	1%
$\tilde{\chi}_1^0\tilde{\chi}_1^0 \to b\bar{b}$	<1%	22%	<1%	80%	<1%
$\tilde{\chi}_1^0\tilde{\chi}_1^0 \to e_3\bar{e}_3$	<1%	1%	<1%	5%	<1%
$\tilde{\chi}_1^0\tilde{\chi}_2^0 \to d\bar{d}$	2.2%	1%	1%	<1%	1%
$\tilde{\chi}_1^0\tilde{\chi}_2^0 \to s\bar{s}$	2.2%	1%	1%	<1%	1%
$\tilde{\chi}_1^0\tilde{\chi}_2^0 \to b\bar{b}$	2.2%	2%	1%	<1%	1%
$\tilde{\chi}_1^0\tilde{\chi}_2^0 \to t\bar{t}$	<1%	<1%	<1%	<1%	1%
$\tilde{\chi}_3^0\tilde{\chi}_2^0 \to d\bar{d}$	<1%	<1%	1%	<1%	<1%
$\tilde{\chi}_3^0\tilde{\chi}_2^0 \to s\bar{s}$	<1%	<1%	1%	<1%	<1%
$\tilde{\chi}_3^0\tilde{\chi}_2^0 \to b\bar{b}$	<1%	<1%	1%	<1%	<1%
$\tilde{\chi}_1^0\tilde{\chi}_2^0 \to u\bar{u}$	1.7%	1%	<1%	<1%	1%
$\tilde{\chi}_1^0\tilde{\chi}_2^0 \to c\bar{c}$	1.7%	1%	<1%	<1%	1%
$\tilde{\chi}_3^0\tilde{\chi}_2^0 \to u\bar{u}$	1.7%	1%	<1%	<1%	<1%
$\tilde{\chi}_3^0\tilde{\chi}_2^0 \to c\bar{c}$	1.7%	1%	<1%	<1%	<1%
$\tilde{\chi}_2^0\tilde{\chi}_2^0 \to W^+W^-$	1.1%	<1%	<1%	<1%	<1%
$\tilde{\chi}_1^+\tilde{\chi}_1^- \to W^+W^-$	2.7%	1%	2%	<1%	2%
$\tilde{\chi}_1^+\tilde{\chi}_1^- \to u\bar{u}$	2.1%	1%	2%	<1%	2%
$\tilde{\chi}_1^+\tilde{\chi}_1^- \to c\bar{c}$	2.1%	1%	2%	<1%	2%
$\tilde{\chi}_1^+\tilde{\chi}_1^- \to t\bar{t}$	2.1%	1%	2%	<1%	2%
$\tilde{\chi}_1^+\tilde{\chi}_1^- \to d\bar{d}$	1.4%	<1%	1%	<1%	1%
$\tilde{\chi}_1^+\tilde{\chi}_1^- \to s\bar{s}$	1.4%	<1%	1%	<1%	1%
$\tilde{\chi}_1^+\tilde{\chi}_1^- \to b\bar{b}$	1.3%	4%	1%	<1%	1%
$\tilde{\chi}_1^+\tilde{\chi}_1^- \to e_1\bar{e}_1$	1.1%	<1%	<1%	<1%	<1%
$\tilde{\chi}_1^+\tilde{\chi}_1^- \to e_2\bar{e}_2$	1.1%	<1%	<1%	<1%	<1%
$\tilde{\chi}_1^+\tilde{\chi}_1^- \to e_3\bar{e}_3$	1.1%	<1%	<1%	<1%	<1%

TABLE III. The co-annihilation channels that contribute to $(\Omega h^2)^{-1}$ for the five benchmarks points chosen in this study. There are many other contributing channels taking the total up to 100% for each benchmark, but for the sake of brevity they are not included in this table if they do not contribute at least 1% for at least one benchmark point.

Centre of Excellence for Particle Physics at the Terascale (CoEPP) (CE110001104). MJW is supported by the Australian Research Council Future Fellowship FT14010024

[1] J.L. Hewett, T.G. Rizzo, Phys. Rept. **183** (1989) 193.

[2] J. F. Gunion, H. E. Haber, G. L. Kane, S. Dawson, "The Higgs Hunter's Guide" (Westview Press, 2000) [Erratum arXiv:hep-ph/9302272];

[3] U. Ellwanger, C. Hugonie and A. M. Teixeira, Phys. Rept. **496**, 1 (2010) [arXiv:0910.1785 [hep-ph]].

[4] M. Maniatis, Int. J. Mod. Phys. A **25**, 3505 (2010) [arXiv:0906.0777 [hep-ph]].

[5] Y. Daikoku, D. Suematsu, Phys. Rev. D **62** (2000) 095006.

[6] J. H. Kang, P. Langacker, T. J. Li, Phys. Rev. D **71** (2005) 015012.

[7] E. Ma, Phys. Lett. B **380** (1996) 286.

[8] E. Ma, M. Raidal, J. Phys. G **28** (2002) 95; J. Kang, P. Langacker, T.-J. Li, T. Liu, Phys. Rev. Lett. **94** (2005) 061801.

[9] J. A. Grifols, J. Sola, A. Mendez, Phys. Rev. Lett. **57** (1986) 2348; D. A. Morris, Phys. Rev. D **37** (1988) 2012.

[10] D. Suematsu, Mod. Phys. Lett. A **12** (1997) 1709.

[11] D. Suematsu, Phys. Rev. D **57** (1998) 1738.

[12] E. Keith, E. Ma, Phys. Rev. D **54** (1996) 3587.

[13] A. Gutierrez-Rodriguez, M. A. Hernandez-Ruiz and M. A. Perez, Int. J. Mod. Phys. A **22**, 3493 (2007) [arXiv:hep-ph/0611235].

[14] D. Suematsu, Phys. Lett. B **416** (1998) 108.

[15] S. W. Ham, J. O. Im, E. J. Yoo and S. K. Oh, JHEP **0812**, 017 (2008) [arXiv:0810.4194 [hep-ph]].

[16] V. Barger, P. Langacker, G. Shaughnessy, New J. Phys. **9** (2007) 333.

[17] M. Asano, T. Kikuchi and S. G. Kim, arXiv:0807.5084 [hep-ph].

[18] B. Stech and Z. Tavartkiladze, Phys. Rev. D **77**, 076009 (2008) [arXiv:0802.0894 [hep-ph]].

[19] V. Barger, P. Langacker, H. S. Lee, G. Shaughnessy, Phys. Rev. D **73** (2006) 115010. J. F. Gunion, L. Roszkowski, H. E. Haber, Phys. Rev. D **38** (1988) 105.

[20] E. Accomando, A. Belyaev, L. Fedeli, S. F. King, C. Shepherd-Themistocleous, Phys. Rev. D **83** (2011) 075012 [arXiv:1010.6058 [hep-ph]].

[21] S. Hesselbach, F. Franke, H. Fraas, Eur. Phys. J. C **23** (2002) 149; V. Barger, P. Langacker, H. S. Lee, Phys. Lett. B **630** (2005) 85; S. Y. Choi, H. E. Haber, J. Kalinowski, P. M. Zerwas, Nucl. Phys. B **778** (2007) 85; V. Barger, P. Langacker, I. Lewis, M. McCaskey, G. Shaughnessy and B. Yencho, Phys. Rev. D **75** (2007) 115002.

[22] T. Gherghetta, T. A. Kaeding, G. L. Kane, Phys. Rev. D **57** (1998) 3178 [hep-ph/9701343].

[23] P. Binetruy, S. Dawson, I. Hinchliffe, M. Sher, Nucl. Phys. B **273** (1986) 501; J. R. Ellis, K. Enqvist, D. V. Nanopoulos, F. Zwirner, Mod. Phys. Lett. A **1** (1986) 57. L. E. Ibanez, J. Mas, Nucl. Phys. B **286** (1987) 107; J. F. Gunion, L. Roszkowski, H. E. Haber, Phys. Lett. B **189** (1987) 409; H. E. Haber, M. Sher, Phys. Rev. D **35** (1987) 2206; J. R. Ellis, D. V. Nanopoulos, S. T. Petcov, F. Zwirner, Nucl. Phys. B **283** (1987) 93; M. Drees, Phys. Rev. D **35** (1987) 2910;

[24] J. Kang, P. Langacker, B. D. Nelson, Phys. Rev. D **77** (2008) 035003 [arXiv:0708.2701 [hep-ph]].

[25] P. Langacker, J. Wang, Phys. Rev. D **58** (1998) 115010.

[26] M. Cvetič, P. Langacker, Phys. Rev. D **54** (1996) 3570; M. Cvetič, P. Langacker, Mod. Phys. Lett. A **11** (1996) 1247; M. Cvetic, D. A. Demir, J. R. Espinosa, L. L. Everett and P. Langacker, Phys. Rev. D **56** (1997) 2861 [Erratum-ibid. D **58** (1998) 119905].

[27] D. Suematsu, Y. Yamagishi, Int. J. Mod. Phys. A **10** (1995) 4521.

[28] E. Keith, E. Ma, Phys. Rev. D **56** (1997) 7155.

[29] P. Athron, D. Harries and A. G. Williams, Phys. Rev. D **91**, 115024 (2015) doi:10.1103/PhysRevD.91.115024 [arXiv:1503.08929 [hep-ph]].

[30] S. F. King, S. Moretti, R. Nevzorov, Phys. Rev. D **73** (2006) 035009.

[31] S. F. King, S. Moretti, R. Nevzorov, Phys. Lett. B **634** (2006) 278.

[32] P. Athron, J. P. Hall, R. Howl, S. F. King, D. J. Miller, S. Moretti and R. Nevzorov, Nucl. Phys. Proc. Suppl. **200-202**, 120 (2010).

[33] R. Howl, S. F. King, JHEP **0801** (2008) 030 [arXiv:0708.1451 [hep-ph]];

[34] F. Braam, J. Reuter and D. Wiesler, AIP Conf. Proc. **1200**, 458 (2010) [arXiv:0909.3081 [hep-ph]].

[35] F. Braam, A. Knochel and J. Reuter, JHEP **1006**, 013 (2010) [arXiv:1001.4074 [hep-ph]].

[36] R. Nevzorov, Phys. Rev. D **87**, 015029 (2013) [arXiv:1205.5967 [hep-ph]].

[37] R. Nevzorov, Phys. Rev. D **89**, no. 5, 055010 (2014) doi:10.1103/PhysRevD.89.055010 [arXiv:1309.4738 [hep-ph]].

[38] P. Athron, M. Mhlleitner, R. Nevzorov and A. G. Williams, JHEP **1501**, 153 (2015) doi:10.1007/JHEP01(2015)153 [arXiv:1410.6288 [hep-ph]].

[39] T. Hambye, E. Ma, M. Raidal, U. Sarkar, Phys. Lett. B **512** (2001) 373.

[40] S. F. King, R. Luo, D. J. Miller, R. Nevzorov, JHEP **0812** (2008) 042.

[41] S. F. King, S. Moretti, R. Nevzorov, Phys. Lett. B **650** (2007) 57 [arXiv:hep-ph/0701064].

[42] R. Howl and S. F. King, Phys. Lett. B **652**, 331 (2007) [arXiv:0705.0301 [hep-ph]].

[43] R. Nevzorov, S. Pakvasa, Phys. Lett. B **728** (2014) 210 [arXiv:1308.1021 [hep-ph]]. J. F. Gunion, L. Roszkowski, H. E. Haber, Phys. Lett. B **189** (1987) 409; H. Baer, D. Dicus, M. Drees, X. Tata, Phys. Rev. D **36** (1987) 1363; S. F. King, S. Moretti, R. Nevzorov, arXiv:hep-ph/0601269; S. Kraml *et al.* (eds.),

Workshop on CP studies and non-standard Higgs physics, CERN–2006–009, hep-ph/0608079; S. F. King, S. Moretti, R. Nevzorov, AIP Conf. Proc. **881** (2007) 138;

[44] J. P. Hall, S. F. King, R. Nevzorov, S. Pakvasa, M. Sher, Phys. Rev. D **83** (2011) 075013 [arXiv:1012.5114 [hep-ph]]; J. P. Hall, S. F. King, R. Nevzorov, S. Pakvasa, M. Sher, arXiv:1012.5365 [hep-ph]; J. P. Hall, S. F. King, R. Nevzorov, S. Pakvasa, M. Sher, arXiv:1109.4972 [hep-ph].

[45] P. Athron *et al.*, arXiv:0810.0617 [hep-ph].

[46] P. Athron, S. F. King, D. J. Miller, S. Moretti, R. Nevzorov, Phys. Lett. B **681** (2009) 448 [arXiv:0901.1192 [hep-ph]].

[47] P. Athron, S. F. King, D. J. Miller, S. Moretti, R. Nevzorov, Phys. Rev. D **80** (2009) 035009 [arXiv:0904.2169 [hep-ph]];

[48] P. Athron, S. F. King, D. J. Miller, S. Moretti, R. Nevzorov, Phys. Rev. D **84** (2011) 055006 [arXiv:1102.4363 [hep-ph]];

[49] P. Athron, S. F. King, D. J. Miller, S. Moretti, R. Nevzorov, Phys. Rev. D **86** (2012) 095003 [arXiv:1206.5028 [hep-ph]].

[50] P. Athron, M. Binjonaid and S. F. King, Phys. Rev. D **87**, no. 11, 115023 (2013) [arXiv:1302.5291 [hep-ph]].

[51] P. Athron, D. Stockinger, A. Voigt, Phys. Rev. D **86** (2012) 095012 [arXiv:1209.1470 [hep-ph]].

[52] A. Voigt,

[53] T. G. Rizzo, Phys. Rev. D **85**, 055010 (2012) [arXiv:1201.2898 [hep-ph]].

[54] D. J. Miller, A. P. Morais and P. N. Pandita, Phys. Rev. D **87**, 015007 (2013) [arXiv:1208.5906 [hep-ph]].

[55] M. Sperling, D. Stckinger, A. Voigt, JHEP **1307** (2013) 132 [arXiv:1305.1548 [hep-ph]];

[56] M. Sperling, D. Stckinger and A. Voigt, JHEP **1401**, 068 (2014) [arXiv:1310.7629 [hep-ph]].

[57] W. Chao, arXiv:1411.5575 [hep-ph].

[58] W. Chao, arXiv:1601.00633 [hep-ph].

[59] S. F. King and R. Nevzorov, JHEP **1603**, 139 (2016) doi:10.1007/JHEP03(2016)139 [arXiv:1601.07242 [hep-ph]].

[60] F. Staub *et al.*, Eur. Phys. J. C **76**, no. 9, 516 (2016) doi:10.1140/epjc/s10052-016-4349-5 [arXiv:1602.05581 [hep-ph]].

[61] J. Kalinowski, S. F. King and J. P. Roberts, JHEP **0901**, 066 (2009) doi:10.1088/1126-6708/2009/01/066 [arXiv:0811.2204 [hep-ph]].

[62] J. P. Hall and S. F. King, JHEP **0908**, 088 (2009) [arXiv:0905.2696 [hep-ph]].

[63] D. S. Akerib *et al.* [LUX Collaboration], Phys. Rev. Lett. **112**, 091303 (2014) doi:10.1103/PhysRevLett.112.091303 [arXiv:1310.8214 [astro-ph.CO]].

[64] D. S. Akerib *et al.* [LUX Collaboration], Phys. Rev. Lett. **116**, no. 16, 161301 (2016) doi:10.1103/PhysRevLett.116.161301 [arXiv:1512.03506 [astro-ph.CO]].

[65] D. S. Akerib *et al.*, arXiv:1608.07648 [astro-ph.CO].

[66] P. Athron, D. Harries, R. Nevzorov and A. G. Williams, Phys. Lett. B **760**, 19 (2016) doi:10.1016/j.physletb.2016.06.040 [arXiv:1512.07040 [hep-ph]].

[67] P. Athron, D. Harries, R. Nevzorov and A. G. Williams, arXiv:1610.03374 [hep-ph].

[68] J. P. Hall and S. F. King, JHEP **1106**, 006 (2011) [arXiv:1104.2259 [hep-ph]].

[69] P. Langacker, Rev. Mod. Phys. **81** (2009) 1199 [arXiv:0801.1345 [hep-ph]].

[70] R. Howl and S. F. King, Phys. Lett. B **687**, 355 (2010) [arXiv:0908.2067 [hep-ph]].

[71] F. Feroz, M. P. Hobson, & M. Bridges, Mon. Not. Roy. Astron. Soc. **398**, 1601 (2009). [arXiv:0809.3437 [astro-ph]]

[72] F. Feroz & M. P. Hobson, Mon. Not. Roy. Astron. Soc. **384**, 449 (2008). [arXiv:0704.3704 [astro-ph]]

[73] F. Feroz, M. P. Hobson, E. Cameron, & A. N. Pettitt, (2013). [arXiv:1306.2144 [astro-ph.IM]]

[74] S. Chatrchyan, V. Khachatryan, A. M. Sirunyan, *et al.*, Physics Letters B, **716**, 30 (2012). [arXiv:1207.7235 [hep-ex]]

[75] ATLAS & CMS Collaborations, (2015). [arXiv:1503.07589 [hep-ex]]

[76] Planck Collaboration, P. A. R. Ade, N. Aghanim, *et al.*, Astron. Astrophys. **571**, A16 (2014). [arXiv:1303.5076 [astro-ph]]

[77] P. Athron, J. h. Park, D. Stckinger, & A. Voigt, Comput. Phys. Commun. **190**, 139 (2015). [arXiv:1406.2319 [hep-ph]]

[78] P. Athron, J. h. Park, D. Stckinger and A. Voigt, Nucl. Part. Phys. Proc. **273-275**, 2424 (2016) doi:10.1016/j.nuclphysbps.2015.09.413 [arXiv:1410.7385 [hep-ph]].

[79] F. Staub, Comput. Phys. Commun. **185**, 1773 (2014). [arXiv:1309.7223 [hep-ph]]

[80] F. Staub, Comput. Phys. Commun. **182**, 808 (2011) doi:10.1016/j.cpc.2010.11.030 [arXiv:1002.0840 [hep-ph]].

[81] F. Staub, Comput. Phys. Commun. **181**, 1077 (2010) doi:10.1016/j.cpc.2010.01.011 [arXiv:0909.2863 [hep-ph]].

[82] F. Staub, Comput. Phys. Commun. **184**, 1792 (2013) doi:10.1016/j.cpc.2013.02.019 [arXiv:1207.0906 [hep-ph]].

[83] F. Staub, Comput. Phys. Commun. **185**, 1773 (2014) doi:10.1016/j.cpc.2014.02.018 [arXiv:1309.7223 [hep-ph]].

[84] B. C. Allanach, Comput. Phys. Commun. **143**, 305 (2002) [hep-ph/0104145].

[85] B. C. Allanach, P. Athron, L. C. Tunstall, A. Voigt and A. G. Williams, Comput. Phys. Commun. **185**, 2322 (2014) doi:10.1016/j.cpc.2014.04.015 [arXiv:1311.7659 [hep-ph]].

[86] M. D. Goodsell, K. Nickel and F. Staub, Eur. Phys. J. C **75**, no. 1, 32 (2015) doi:10.1140/epjc/s10052-014-3247-y [arXiv:1411.0675 [hep-ph]].

[87] J. Pardo Vega and G. Villadoro, JHEP **1507**, 159 (2015) doi:10.1007/JHEP07(2015)159 [arXiv:1504.05200 [hep-ph]].

[88] G. Belanger, F. Boudjema, A. Pukhov and A. Semenov, arXiv:1005.4133 [hep-ph].

[89] G. Belanger, F. Boudjema, A. Pukhov and A. Semenov, arXiv:0803.2360 [hep-ph].

[90] G. Belanger, F. Boudjema, A. Pukhov and A. Semenov, Comput. Phys. Commun. **176** (2007) 367 [arXiv:hep-ph/0607059].

[91] P. Athron, J. h. Park, T. Steudtner, D. Stckinger and A. Voigt, arXiv:1609.00371 [hep-ph].

[92] A. Belyaev, N. D. Christensen and A. Pukhov, Comput. Phys. Commun. **184**, 1729 (2013) doi:10.1016/j.cpc.2013.01.014 [arXiv:1207.6082 [hep-ph]].

[93] A. Semenov, arXiv:1005.1909 [hep-ph].

[94] A. Belyaev, J. P. Hall, S. F. King and P. Svantesson, Phys. Rev. D **86**, 031702 (2012) doi:10.1103/PhysRevD.86.031702 [arXiv:1203.2495 [hep-ph]].

[95] A. Belyaev, J. P. Hall, S. F. King and P. Svantesson, Phys. Rev. D **87**, no. 3, 035019 (2013) doi:10.1103/PhysRevD.87.035019 [arXiv:1211.1962 [hep-ph]].

[96] N. Arkani-Hamed, A. Delgado and G. F. Giudice, Nucl. Phys. B **741**, 108 (2006) doi:10.1016/j.nuclphysb.2006.02.010 [hep-ph/0601041].

[97] E. Aprile, J. Aalbers, F. Agostini, et al. Journal of Cosmology and Astroparticle Physics, **4**, 027 (2016). [arXiv:1512.07501 [physics.ins-det]]